Available online at www.sciencedirect.com
ScienceDirect
Chemical Physics Letters 446 (2007) 103–108
CHEMICAL PHYSICS LETTERS
www.elsevier.com/locate/cplett

Raman and conductivity studies of boron doped microcrystalline diamond, facetted nanocrystalline diamond and cauliflower diamond films

P.W. May [a,*], W.J. Ludlow [a], M. Hannaway [a], P.J. Heard [b], J.A. Smith [a], K.N. Rosser [a]

[a] School of Chemistry, University of Bristol, Bristol BS8 1TS, UK
[b] Interface Analysis Centre, University of Bristol, Oldbury House, 121 St Michael's Hill, Bristol BS2 8BS, UK

Received 30 May 2007; in final form 3 August 2007
Available online 11 August 2007

Abstract

We present data showing how the electrical conductivity and Raman spectra of boron-doped CVD diamond films vary with both B content and crystallite size, for microcrystalline diamond (MCD), facetted nanocrystalline diamond (f-NCD) and 'cauliflower' diamond (c-NCD). The position of the Lorentzian contribution to the 500 cm^{-1} Raman feature was used to estimate the B content. This underestimated the SIMS concentration of B by a factor of ~5 for the f-NCD and c-NCD films, but remained reasonably accurate for MCD films. One explanation for this is that most of the B incorporates at the grain boundaries and not in substitutional sites.

1. Introduction

Diamond films produced by chemical vapour deposition (CVD) can be doped with boron to produce a p-type semiconducting material with electrical conductivity that ranges from insulating to metallic, depending upon the doping level [1], and therefore show great promise for use in a variety of electronic devices. The boron dopant atoms act as electron acceptors, and form a band located ~0.35 eV above the valence band edge. At low temperatures or at boron concentrations $<10^{17}$ cm^{-3} conduction occurs through holes in the valence band contributed by ionised substitutional B. At higher doping levels, conduction occurs by nearest-neighbour and variable range hopping of holes between ionised B sites [2], accompanied by a drop in mobility [3]. At very high doping levels, an impurity band is formed, giving rise to metal-like conductivity, and even superconductivity at temperatures <4 K [4].

A complication is that polycrystalline boron-doped CVD diamond films possess grain boundaries containing a small-volume fraction of non-diamond carbon impurities. Consequently, the electrical conductivity of the film is a complicated function of the combined effects of the boron-doping level, the grain boundaries, and the impurities. As the grain size in the films becomes smaller, *i.e.* from microcrystalline diamond (MCD) to nanocrystalline diamond (NCD), the relative importance of these grain boundaries increases. As a result, most reports concerning B-doped diamond, both fundamental science-based and applications-led, have concentrated upon epitaxially-grown diamond or large-grained MCD films. There have been relatively few studies concerning B-doped NCD films, with the majority concerning their applications for electrochemical electrodes [5] or other devices [6,7]. However, a recent theoretical study by Barnard and Sternberg [8] predicted that boron is likely to be preferentially located at the surface of isolated diamond nanoparticles and at the grain boundaries in NCD films – which has serious implications for the conduction properties of such films, and hence their utility in electronic devices.

* Corresponding author. Fax: +44 (0)117 9251295.
E-mail address: paul.may@bris.ac.uk (P.W. May).

0009-2614/$ - see front matter © 2007 Elsevier B.V. All rights reserved.
doi:10.1016/j.cplett.2007.08.018

Unfortunately, there is no rigorous definition for NCD in the literature, and the only agreed property is that the films have grain sizes in the nm range, typically between 10 and 500 nm. In fact, a number of films with quite distinct characteristics all come under the broad umbrella of NCD [9]. One type of NCD film is deposited if the deposition occurs with a very high initial nucleation density (*e.g.* by using nanodiamond grit for abrasion), followed by standard growth conditions [10]. These films exhibit columnar growth, just as for MCD, except with nano-sized crystallites. There is little or no re-nucleation, and the grain size, and hence roughness, increase with film thickness, so that above a thickness of around 1 μm, the film becomes microcrystalline. Thus, these NCD films can be considered as just smaller grained, facetted versions of MCD, and we shall refer to them as 'facetted NCD' (f-NCD).

However, this description is not appropriate for many other NCD films, which often contain a significant fraction of non-diamond material, and exhibit no faceting or evidence of columnar growth, even at thicknesses of several μm. Some NCD films have a rounded appearance and as a result, their morphology is often referred to as 'ballas' (meaning ball-like) or cauliflower-like [11,12]. We shall call these types of films 'cauliflower NCD' (c-NCD). Thicker c-NCD films can be grown with essentially flat surfaces with nm smoothness, and this allows them to be patterned with much higher resolution than MCD. Decreasing the diamond crystallite size below 10 nm produces what has come to be known as 'ultrananocrystalline' diamond (UNCD) films [13]. However, there are as yet no reports of successful B-doping of UNCD [14].

Studies of the Raman spectra from B-doped diamond films have also been restricted almost exclusively to epitaxial or MCD films [15]. The diamond phonon observed at 1332 cm^{-1} is a symmetric Lorentzian at low boron concentration, but as the boron concentration increases above a threshold of $\sim 10^{20}$ cm^{-3} – corresponding to the onset of metallic conductivity – there is an abrupt and pronounced change toward an asymmetric Fano-like lineshape [16]. This is caused by a quantum mechanical interference between the zone-centre Raman-active optical phonon and the continuum of electronic states induced by the presence of the dopant. The threshold for the appearance of the Fano-like lineshape was found to depend on the excitation laser wavelength [17]. The Raman peak also shifts to lower wavenumber with increased boron concentration, and is accompanied by a wide signal (300–1330 cm^{-1}) with structures around 500 and 1225 cm^{-1} (although these structures do not appear when using ultraviolet (244 cm^{-1}) excitation [18]). Such results were first reported for epitaxially-grown diamond [19,20] and then confirmed [16,21] for polycrystalline boron-doped MCD films. Wang et al. [18] found that this shift in the peak position was also a function of excitation wavelength in the range 244–514 nm. The origin of the peaks 500 and 1225 cm^{-1} peaks is uncertain, but the positions of these two bands agree with two maxima in the phonon density of states (PDOS). They may therefore be connected with a relaxation of the wavevector selection rules, and if so, they may well be associated with the actual boron incorporation in the lattice, rather than the hole concentration [22]. There is also evidence [23] that the 500 cm^{-1} peak originates from local vibrational modes of boron pairs [24], which cause some distortion in the diamond lattice around these isolated defects.

For very heavy B-doping, the Fano parameters saturate and it becomes difficult to discern the position of the zone-centre phonon, with the peaks at 500 and 1225 cm^{-1} dominating the spectrum. For these conditions, the 500 cm^{-1} peak can be fitted with a combination of Gaussian and Lorentzian line shapes, and the wavenumber, ω, of the Lorentzian component approximately obeys [22]:

$$[\mathrm{B}]/\mathrm{cm}^{-3} = 8.44 \times 10^{30} \exp(-0.048\omega) \quad (1)$$

where ω is in cm^{-1} and the boron content, [B], is in the range from 2×10^{20} to 1×10^{22} cm^{-3}.

2. Experimental

The three types of diamond film were all grown in a standard hot filament CVD reactor using CH_4/H_2 process gases at a pressure of 20 Torr. The substrate was undoped single crystal (1 0 0) Si, abraded ultrasonically before deposition using a slurry of 100 nm diamond grit in water. Rhenium was used for the filament material rather than tantalum since Re does not act as a sink for carbon or boron species, unlike Ta which can absorb significant amounts of B and C for many hours into the deposition run [25]. The filament temperature was kept constant at 2400 °C and monitored using a 2-colour optical pyrometer, and the substrate temperature was maintained at ~900 °C. Diborane (B_2H_6) gas diluted in H_2 was used as the source of B at concentrations between 10 and 12 000 ppm with respect to CH_4. All three gases were metered into the chamber using mass flow controllers.

For MCD and f-NCD, a ratio of 1%CH_4/H_2 was used, whereas for c-NCD the methane concentration was increased to 5%. The only difference between MCD and f-NCD was that for f-NCD the ultrasonic abrasion was performed for much longer to ensure high nucleation density, and the film growth was stopped after 90 min to give a continuous film <1 μm thick with small facetted grains. MCD and c-NCD films were grown for 8 h giving films ~4 μm thick. The various film morphologies can be seen in Fig. 1. Undoped films were grown in a different but otherwise identical HF CVD reactor that had never had boron introduced into it. This is because B is known to diffuse into the sidewalls and components within a reactor, and then diffuse out again during later growth runs, inadvertently introducing B into the gas mixture and causing unwanted doping of any growing film. With increasing B content, the films became visibly darker, and had a bluish tinge.

All measurements were made on the as grown films, with no post-growth treatments (*e.g.* high temperature oxida-

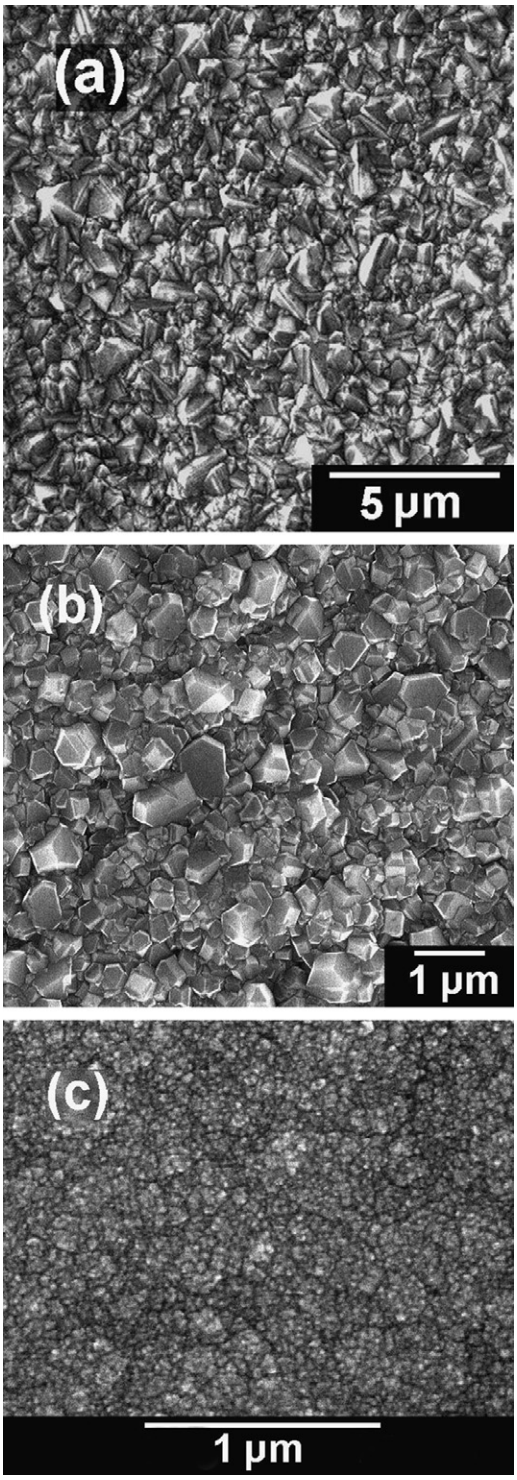

Fig. 1. Scanning electron micrographs of the surface of (a) MCD, showing randomly-oriented grain sizes around 0.5–1 μm, (b) f-NCD, with grain sizes ~100–500 nm, and (c) c-NCD, with grains sizes 20–100 nm.

tion in air) taking place. Electrical conductivity measurements were made by 4-point probe methods. In these, spring-loaded probes were pressed into contact with the surface of the film and the resistance measured over a distance of ~5 mm. Note that even though the 4-point probe measurements supposedly remove most of the effects of contact resistance, these measurements were of the effective surface conductivity, and might not correspond to the bulk conductivity. Linear plots of current against applied voltage, passing through the origin, were obtained, showing that the contacts were Ohmic. Boron content within the film was measured using secondary ion mass spectrometry (SIMS), with the B:C count ratio being calibrated with respect to those from two reference samples. The first reference was a single crystal diamond implanted with a known dosage of B, and therefore containing a known B-content. The second reference was an undoped CVD diamond film with zero B content, providing the background count level for B. Metallic impurities, such as tantalum from the filament or Mo from the substrate holder, which might contribute to film conductivity were not seen at the detection limit of the SIMS.

Laser Raman spectra were obtained at room temperature using a Renishaw 2000 spectrometer and a range of excitation wavelengths and lasers: UV 325 nm (HeCd), blue 488 nm (Ar^+), green 514 nm (Ar^+), red 625 nm (HeNe), IR 785 nm (IR diode), and far-IR 830 nm (IR-diode). Undoped or lightly doped films often exhibited a large rising or falling photoluminescent (PL) background upon which the much smaller Raman features would sit. This PL background would decrease markedly with even trace amounts of B doping, and for B contents $>5\times10^{18}$ cm^{-3} it disappeared altogether giving a flat baseline. In order to see the small Raman features more clearly, and to reproduce the spectra from the undoped films on the same scale as the doped ones, it was useful to subtract this PL background where necessary.

In those spectra where the 500 cm^{-1} band was discernible (*i.e.* from the more heavily doped samples), the band was fitted to a combination of a Gaussian curve centred ~500–550 cm^{-1} and a Lorentzian curve centred ~460–505 cm^{-1} following the procedure outlined in Ref. [22]. Using the relationship between the B content and the wavenumber of the Lorentzian component of the 500 cm^{-1} band Eq. (1), it was possible to estimate the doping levels in these films, with which to compare the values obtained using SIMS.

3. Results

To investigate the behaviour of the different types of B-doped CVD diamond film, a range of MCD, f-NCD and c-NCD films were deposited onto Si substrates and their doping levels and resistance values are given in Table 1. Electron micrographs of their surface morphologies can be seen in Fig. 1. The values of the boron content in the films are plotted against 4-point conductance (=1/resistance) in Fig. 2. The trends are roughly linear for all three film types, but the conductance of the MCD films is significantly higher than those for the other two films, for the same apparent B content. We note that the conductivity of c-NCD films did not begin to rise significantly until

Table 1
B content as measured by SIMS, and as estimated from fitting the 500 cm^{-1} Raman peak using Eq. (1), plus 4-point resistance measurements for the three types of films

	B content/cm^{-3} (SIMS)	B content/cm^{-3} (Raman fit)	4-Point resistance/Ω
MCD films			
M1	0	–	7600
M2	2.4×10^{19}	–	1550
M3	7.5×10^{19}	–	500
M4	3.7×10^{20}	3.0×10^{20}	81
M5	*6.0×10^{20}*	4.0×10^{20}	52
M6	1.5×10^{21}	7.2×10^{20}	20
M7	*2.3×10^{21}*	1.4×10^{21}	9
f-NCD films			
F1	0	–	9.0×10^{4}
F2	1.5×10^{20}	–	3800
F3	1.4×10^{20}	–	3700
F4	*5.0×10^{20}*	–	1000
F5	1.3×10^{21}	2.6×10^{20}	121
F6	2.4×10^{21}	3.0×10^{20}	95
F7	2.8×10^{21}	8.7×10^{20}	67
c-NCD films			
C1	0	–	1×10^{7}
C2	6.0×10^{18}	–	5×10^{6}
C3	6.1×10^{20}	–	6480
C4	1.1×10^{21}	3.4×10^{20}	294
C5	2.9×10^{21}	4.5×10^{20}	66
C6	6.1×10^{21}	9.6×10^{20}	43

The italicised values for SIMS B content for M5, M7 and F4 indicates that these were not measured directly, but were interpolated from the plot in Fig. 2.

the doping level had reached 5×10^{20} cm^{-3}. This suggests that a grain-boundary-related impurity, such as hydrogen, may be passivating the boron up to this concentration.

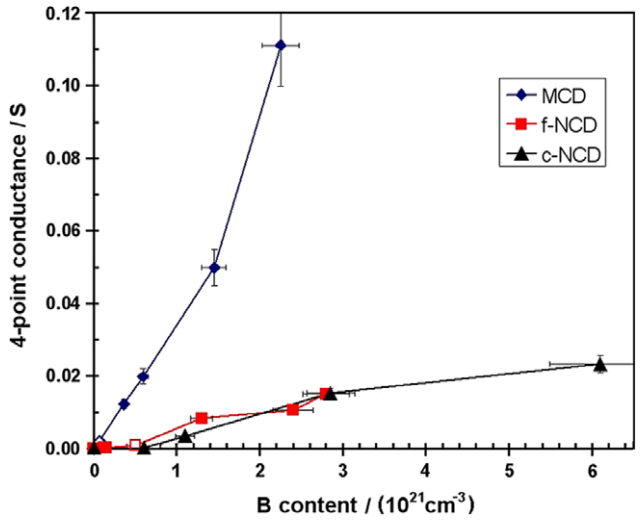

Fig. 2. B content plotted against measured 4-point conductance (1/resistance) for the three types of films. Filled points are the values of B content in the films measured by SIMS, the hollow points are estimated values of B content based on inter/extrapolation of the trends from the other points. B content values are estimated to be accurate to ±10%, as shown by error bars.

However, this would be a minor offset when dealing with the much higher doping levels.

For brevity, we shall restrict ourselves to compare the Raman spectra of only the heaviest B-doped films as a function of excitation wavelength (Fig. 3). For the heavily B-doped MCD film (M7), the UV spectrum is clearly different in form to the others, exhibiting features at 800 and 1050 cm^{-1}, as well as the G peak (from ordered graphitic structures) at 1550 cm^{-1} which do not appear in the other spectra. For all the other spectra taken at longer wavelengths, there is a clear trend with the 1225 cm^{-1} peak gradually shifting to higher wavenumber, whilst the diamond peak shifts to lower wavenumber and broadens. This behaviour is due to the Fano resonance effects mentioned earlier. The relative intensity of the 500 cm^{-1} peak increases with increasing laser wavelength. This is also true for the f-NCD spectra (F7), with the diamond peak well resolved in the UV spectrum, but having merged into the large 1225 cm^{-1} peak in the IR spectrum. For the c-NCD

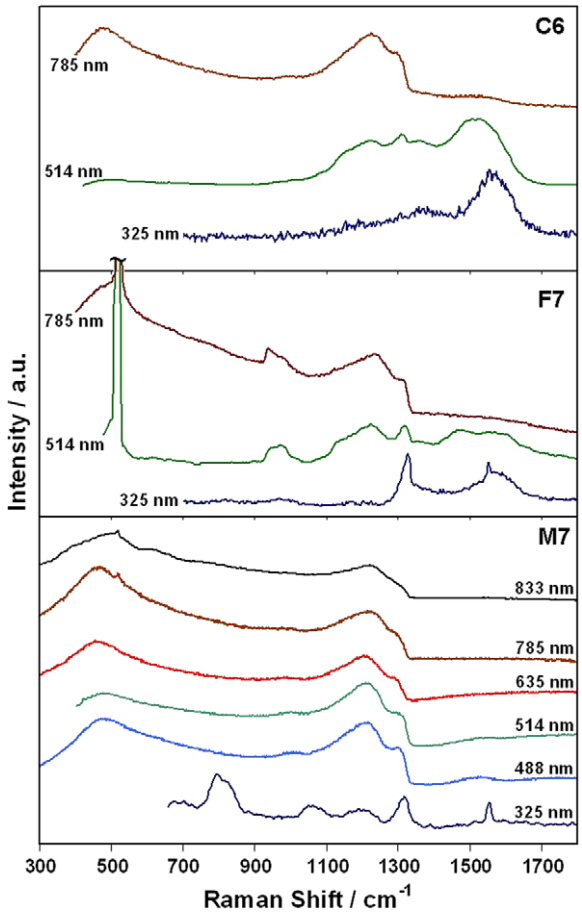

Fig. 3. Raman spectra for the most heavily B-doped of the three types of film, M7, F7 and C6 (details in Table 1), for a range of different laser excitation wavelengths from the UV to the far IR. The spectra have been offset vertically from each other for clarity, with no PL background subtraction (except for F7, 514 nm), and have been scaled in intensity to allow ease of comparison. The large Si peaks at 520 cm^{-1} in F7 (514 and 785 nm) have been truncated for clarity.

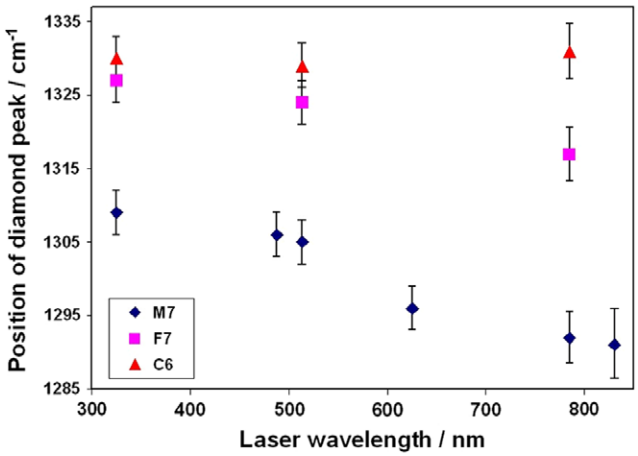

Fig. 4. The position of the diamond Raman peak as a function of excitation wavelength for the three types of heavily B-doped diamond film.

spectra (C6), the diamond peak is not well resolved in either the UV or the green spectra, and is only really apparent as a shoulder on the 1225 cm^{-1} peak in the IR spectrum.

Fig. 4 shows the position of the diamond peak for the heaviest doped samples as a function of excitation wavelength. For the heavily B-doped MCD sample, the peak position shifts to lower wavenumber with increasing laser wavelength, as noted by Wang et al. [18]. For the f-NCD films, this shift is less severe, and for the c-NCD films there is no apparent shift, within the resolution of the Raman spectrometer. This suggests that the Fano-type interference of the diamond line is a function of crystallite size, and for nm-sized crystals the effect is drastically reduced.

Table 1 also shows the values for B concentration for the heavier doped films estimated from the Raman fit of the 500 cm^{-1} peak and Eq. (1). The values for the MCD films are all within a factor of 2 of those measured by SIMS, showing that for MCD films Eq. (1) is quite accurate. However, for the f-NCD films the estimated values are much less accurate, underestimating the SIMS values by factors of between 3 and 10. The same is true for the c-NCD films, where the values underestimate those from SIMS by factors of between 3 and 6. The difference arises since SIMS counts *all* the B present in the film, whereas the Raman method only counts those boron atoms which directly affect the 500 cm^{-1} band.

4. Conclusions

We found that the conductance of B-doped MCD films was much higher than those for the smaller grained films, for the same B content. This suggests that the doping efficiency for MCD films is greater than for the other two types of film, and this might be explained if a greater proportion of the incorporated B atoms were contributing to doping in MCD. In f-NCD and c-NCD films, the reduced doping efficiency suggests that a significant amount of the B is being incorporated in positions which do not improve the conductivity to the same extent as doping the crystallites themselves, such as at the grain boundaries. Such grain boundary 'doping' might still affect the overall film conductivity, since it may provide alternative conduction pathways that compete with the through-grain conduction. This will be explored following more detailed conductivity measurements to appear in subsequent publications.

We also found that the Raman Fano interference effects were much reduced for the smaller grain-sized material, and that Eq. (1) underestimates the concentration of B in the films by a factor of ~5 for the f-NCD and c-NCD films, although it remains reasonably accurate for MCD films. Eq. (1) measures only those boron atoms which directly incorporate into the diamond lattice (and hence affect the position of the 500 cm^{-1} band). The shortfall between these values and the total values measured by SIMS may also be explained if only a small fraction of the B found in the small-grained films is being incorporated into substitutional sites. The majority of the B (80% in some cases) must be present at sites that do not contribute to the continuum of electronic states that give rise to metallic conductivity and the Fano effects. Therefore, it is important to realise when studying conduction or superconduction behaviour in small-grained diamond films that the B content measured by techniques such as SIMS may not be representative of the actual level of substitutional doping of the grains themselves. Nevertheless, despite the complexity of the underlying conduction mechanisms present in f-NCD and c-NCD films, they can be fabricated with controllable conductivities and nm-smooth surfaces, which might make them ideal candidates for use as an electronic material.

Acknowledgements

The authors would like to thank Jacob Filik, Martin Kuball & Tim Batten, and Keith Hallam & Diana Edwards for use of their far IR, blue, and red Raman systems, respectively, and Jonathan Jones for the high resolution SEM photos.

References

[1] R. Kalish, Carbon 37 (1999) 781.
[2] B. Massarani, J.C. Bourgoin, R.M. Chrenko, Phys. Rev. B 17 (1978) 1758.
[3] K. Nishimura, K. Das, J.T. Glass, J. Appl. Phys. 69 (1991) 3142.
[4] E.A. Ekimov et al., Nature 428 (2004) 542.
[5] Yu. V. Pleskov, Russ. J. Electrochem. 38 (2002) 1275.
[6] M. Willander, M. Friesel, Q.-ul. Wahab, B. Straumal, J. Mater. Sci: Mater. Electron. 17 (2006) 1.
[7] D.L. Dreifus, A. Collins, T. Humphreys, K. Das, P.E. Pehrsson (Eds.), Diamond for Electronic Applications, MRS Symp. Proc, vol. 416, Materials Research Society, Pittsburgh, 1996.
[8] A.S. Barnard, M. Sternberg, J. Phys. Chem. B 110 (2006) 19307.
[9] P.W. May, in: A. Öchsner, W. Ahmed (Eds), Carbon Based Nanomaterials, Trans Tech, Switzerland, in press.
[10] O.A. Williams et al., Diam. Relat. Mater. 15 (2006) 654.

[11] E. Kohn, P. Gluche, M. Adamschik, Diam. Relat. Mater. 8 (1999) 934.
[12] F.J.H. Guillen, K. Janischowsky, J. Kusterer, W. Ebert, E. Kohn, Diam. Relat. Mater. 14 (2005) 411.
[13] D.M. Gruen, O.A. Shenderova, A.Ya. Vul' (Eds.), Synthesis, Properties and Applications of Ultrananocrystalline Diamond, NATO Science Series part II, vol. 192, Springer, 2005.
[14] P.W. May, M. Hannaway, Mat. Res. Symp. Proc. PV-956 (2006), 0956-J09-31.
[15] S. Prawer, R.J. Nemanich, Philos. Trans. Roy. Soc. Lond. A 362 (2004) 2537.
[16] J.W. Ager III, W. Walukiewicz, M. McCluskey, M.A. Plano, M.I. Landstrass, Appl. Phys. Lett. 66 (1995) 616.
[17] F. Pruvost, E. Bustarret, A. Deneuville, Diam. Relat. Mater. 9 (2000) 295.
[18] Y.G. Wang, S.P. Lau, B.K. Tay, X.H. Zhang, J. Appl. Phys. 92 (2002) 7253.
[19] E. Gheeraert, P. Gonon, A. Deneuville, L. Abello, G. Lucazeau, Diam. Relat. Mater. 2 (1993) 742.
[20] P. Gonon, E. Gheeraert, A. Deneuville, L. Abello, G. Lucazeau, J. Appl. Phys. 78 (1995) 7059.
[21] R. Locher et al., Diam. Relat. Mater. 4 (1995) 678.
[22] M. Bernard, A. Deneuville, P. Muret, Diam. Relat. Mater. 13 (2004) 282.
[23] M. Bernard, C. Baron, A. Deneuville, Diam. Relat. Mater. 13 (2004) 896.
[24] J.P. Goss, P.R. Briddon, Phys. Rev. B 73 (2006) 085204.
[25] D.W. Comerford et al., J. Phys. Chem. A 110 (2006) 2868.